

Effect of pre-existing substructures on the fatigue properties of pure aluminium

M. T. JAHN, TSANN LIN, C. M. WAN

Department of Materials Science and Engineering, National Tsing Hua University, Hsinchu, Taiwan, Republic of China

Pure aluminium was thermomechanically treated (cold rolled to 80% reduction of thickness and annealed at 200° C for various lengths of time) in order to obtain different kinds of substructures. These aluminium specimens were then fatigued with a stress amplitude of 9×10^3 psi* or 90% of their ultimate tensile strength. The substructures of the specimens before and after fatigue were compared with each other and were then correlated to their fatigue property. The size and shape of substructure introduced by fatigue depend on the pre-existing substructure formed by thermomechanical treatment. The sub-boundaries of the fatigued specimen are not as well-defined as the pre-existing subgrain. The substructure size of the fatigued specimen increases initially with annealing time and then reaches a saturation value ($2.32 \mu\text{m}$) when the annealing time is longer than 2 h. A peak value of fatigue life against the annealing time was found if the stress amplitude of fatigue is 90% of the ultimate tensile strength. The peak value also occurs at an annealing time of 2 h. The reason why the specimen annealed for 2 h possesses the optimum fatigue and property is discussed in terms of the substructures before and after fatigue.

1. Introduction

The familiar thermomechanical treatment is firstly to introduce a high dislocation density by plastic deformation. The dislocation distribution is then rearranged into a more stable substructure by some kind of recovery heat-treatment [1, 2]. The formation of pre-existing substructure in metals by thermomechanical treatment improves the mechanical properties such as tensile strength, yield strength, toughness and fatigue life [2-4]. Since substructures will also be formed after the fatigue process [5, 6] we call the substructures formed by thermomechanical treatment before fatigue the "pre-existing substructures". In general, the increase of fatigue life of a metal with a pre-existing substructure compared to those without pre-existing substructures is because the former possesses greater strength. The detailed mechanisms of how the pre-existing substructure affects the fatigue process have seldom been studied. Jahn *et al.* [4] suggested that pre-existing subgrains may

increase the fatigue life by maintaining a larger subgrain size which leads to less crack propagation routes than in annealed material after fatigue if the fatigue crack propagates along sub-boundaries [7]. It is also suggested by Jahn *et al.* [8] that the fatigue-crack nucleation is more difficult in metals having pre-existing subgrains due to the fact that the strain distribution within the grains is more uniform and the stress gradient at the grain boundaries is reduced by the presence of pre-existing subgrains. The effect of pre-existing substructure on fatigue properties of metals studied before [4, 8] were all concentrated in well-defined subgrains of $\sim 2 \mu\text{m}$ in pure aluminium. Since there are different sizes and kinds of substructure, such as tangled dislocations, dislocation cells and subgrains, one may ask how will the shape and size of pre-existing substructure affect the fatigue properties of metals. So far as we know the above mentioned effects have never been studied before. In this work we obtained dislocation cells (1 to

* 10^3 psi $\equiv 6.89 \text{ N mm}^{-2}$.

TABLE I Composition of the Al specimen (wt %)

Si	Fe	Cu	Pb	Zn	Bi	Sn	Al
0.06	0.004	0.004	0.003	0.003	0.0075	0.0065	balance

2 μm in size) and subgrains (2 to 4 μm in size) in pure Al specimens by various kinds of thermo-mechanical treatment. The fatigue properties and substructures of the specimens before and after fatigue were compared. It is our hope that the information obtained will help to explain the optimum conditions of pre-existing substructure which make the metals possess optimum fatigue properties.

2. Experimental details

Pure aluminium was chosen for this study because it possesses high stacking-fault energy such that various kinds of substructure can be easily formed by thermomechanical treatment or by a fatigue process. The purity of the aluminium investigated was 99.9%. The chemical composition of the samples is given in Table I. Homogenized pure aluminium plates were cold-rolled to 80% reduction ratio in thickness. These rolled sheets were then annealed at 200 or 400°C for various times. Full recrystallization was found in specimens after annealing at 400°C for a time in excess of 0.2 h. These specimens are called F. F 0.2, F 0.5, etc, means specimens F annealed at 400°C for 0.2 h, 0.5 h, etc, respectively. Various kinds and different sizes of substructure were obtained in specimens after annealing at 200°C for various times. These specimens are called S. Specimens S 2.0, S 3.0, etc, represent specimens annealed at 200°C for 2 h, 3 h, etc, respectively. Specimen F possesses no pre-existing substructure before fatigue. All specimens were fatigued by cyclic bending stress

with zero mean stress. The direction of fatigue stress was either perpendicular (transverse) or parallel (longitudinal) to the rolling direction of the specimens. Specimens F were fatigued with a stress amplitude of 6×10^3 psi. Specimens S were fatigued with a stress amplitude of 9×10^3 psi or 90% of their ultimate tensile strength. The fatigue test was carried out in air, at room temperature on a Sonntag model SF-2-U fatigue test machine at a cyclic frequency of 1800 cycles min^{-1} . The microstructures of all specimens before and after fatigue were investigated with a Jeol 100B transmission electron microscope operating at 100 kV. For each fatigued specimen, the region near the fracture surface was carefully cut off. It was then protectively painted on one side of the free surface so that chemical polishing operated from the other side only, and the area under higher stress during fatigue was retained. The TEM thin foil about 2 mm from the fracture surface was prepared by the window method of electropolishing. The TEM micrographs were only taken from the thicker portions of thin foil where dislocations did not escape due to thermal stress. Such a procedure resulted in a lack of resolution and contrast, but the information obtained was more reliable. Each average value of substructure size was measured by the intersection method on at least three TEMs.

3. Experimental results and discussions

Several typical TEMs of specimens S are shown in Figs 1 to 4. Figs 1a to 4a represent the substructures of specimens S before fatigue. Figs 1b to 4b show the corresponding substructures after fatigue. The fatigue conditions and fatigue life of the specimens are given along with the figures. When pure aluminium associated with high stacking-fault

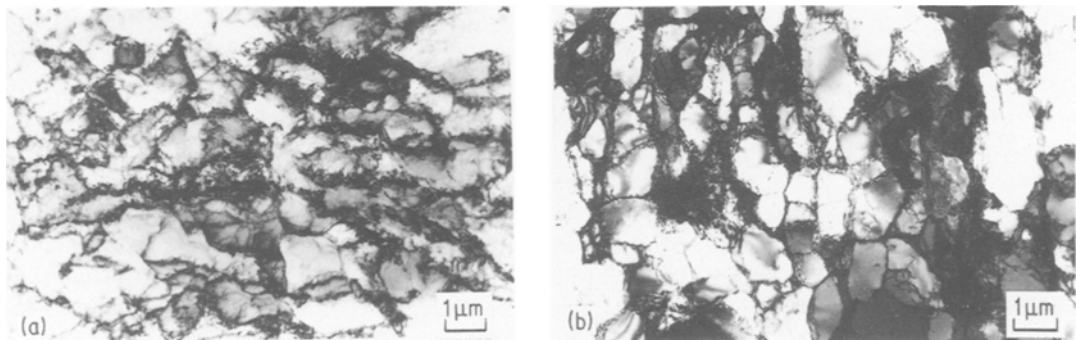


Figure 1 (a) TEM microstructure of as-rolled specimen S 00. (b) TEM microstructure of specimen S 00 after fatigue. Fatigue stress amplitude $\sigma_{\text{ap}} = 9 \times 10^3$ psi. Fatigue life $N_f = 1.44 \times 10^5$ cycles. Transverse direction.

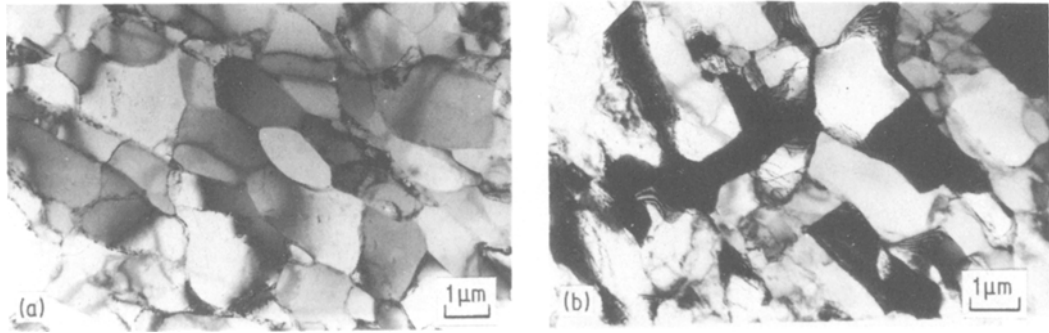


Figure 2 (a) TEM microstructure of specimen S 0.5. (b) TEM microstructure of specimen S 0.5 after fatigue. $\sigma_{ap} = 9 \times 10^3$ psi, $N_f = 1.16 \times 10^5$ cycles. Transverse direction.

energy is being rolled, dislocations will multiply first; cross slip of dislocations then occurs in the stage of dynamic recovery, hence three-dimensional dislocation movement can be operative so that cell formation can be induced.

Fig. 1a shows the substructure in a specimen just after rolling to 80% reduction of thickness. Dislocation cells are nearly formed although the cell boundaries are not well defined and there still exists some dislocation inside the cells. During the annealing of specimens at 200°C, microhardness and strength decrease gradually as a result of static recovery which proceeds by cross slip, climb, combination and annihilation of dislocations. The substructure rearrangement also proceeds by the annihilation of redundant dislocations in cell walls and the attraction of interior dislocations into walls.

Fig. 2a represents the substructure of specimen S 0.5 in which the cell walls become sharper, but are still not well-defined. As walls become sharper and sharper, the cells polygonize into subgrains. Polygonization is complete after annealing the

specimen for 2 h as shown in Fig. 3a. Then the growth of subgrains proceeds by decomposition of weaker sub-boundaries.

Fig. 4a shows decomposition of subgrain boundaries of specimen S 72. Ignoring the ambiguous sub-boundaries, we see that the well-defined subgrain size of specimen S 72 is about 3.69 μm. Repeated deformation of fatigue on specimen S 00 results in a change of substructure due to dynamic recovery during cycling.

Comparing Figs 1a and 1b, one finds that the walls of dislocation cells become sharper and the cell size increases a little after fatigue. For specimen S 0.5 the sharpness of the sub-boundaries remains almost unchanged after fatigue; however, the size of substructure increases slightly after fatigue as shown in Fig. 2a and b. The fact that after fatigue the substructure size becomes larger in specimens S annealed for less than 2 h at 200°C indicates that fatigue softening has occurred. For specimen S 2.0 in which the polygonization is complete, the substructure size remains almost unchanged after fatigue; however, the substructure

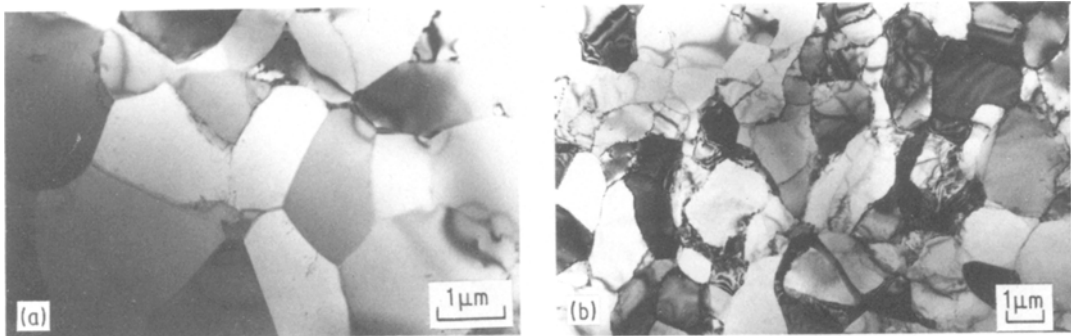


Figure 3 (a) TEM microstructure of specimen S 2.0. (b) TEM microstructure of specimen S 2.0 after fatigue. $\sigma_{ap} = 9 \times 10^3$ psi, $N_f = 6.6 \times 10^4$ cycles. Transverse direction.

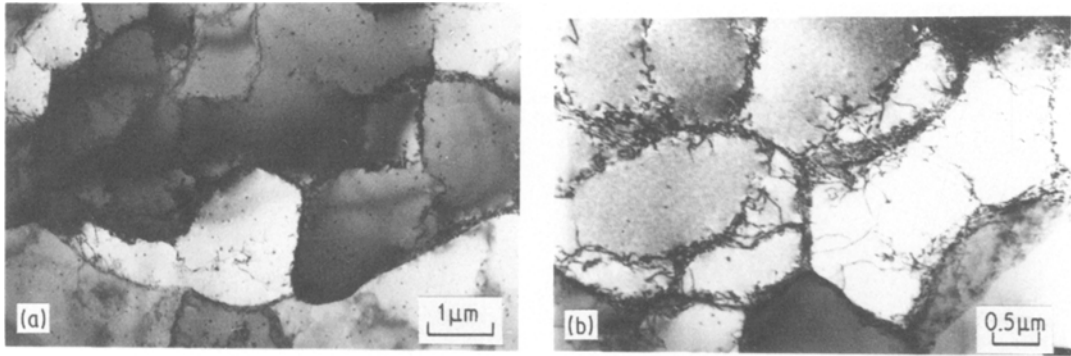


Figure 4 (a) TEM microstructure of specimen S 72. (b) TEM microstructure of specimen S 72 after fatigue. $\sigma_{ap} = 9 \times 10^3$ psi, $N_f = 2.4 \times 10^4$ cycles. Transverse direction.

boundary becomes less well-defined compared to the pre-existing subgrain as shown in Fig. 3a and b. The size of substructure is about $2.32 \mu\text{m}$.

As the annealing time of specimen S is further increased the boundaries of substructures become less and less defined; however, after fatigue the substructure size reaches a saturation value ($2.32 \mu\text{m}$) as shown in Fig. 4a and b. The relationship between the size of substructure of specimen S before and after fatigue, respectively, and the annealing time, is plotted in Fig. 5. The extent of final saturation cell size is evidently the mean free path of dislocations. When cell formation is

complete, further deformation in the saturation hardening stage must proceed by pumping dislocations into cell walls so that strain can be accommodated by this flip-flop motion of dislocations. This mechanism can be confirmed by the existence of individual dislocations inside fatigue-induced cells as shown in Fig. 4b.

The relationship between the ultimate tensile strength (UTS) of specimens S and F and the annealing time is shown in Fig. 6. The ultimate tensile strength of specimen S decreased monotonically with increasing annealing time. Longitudinal and transverse specimens possess similar

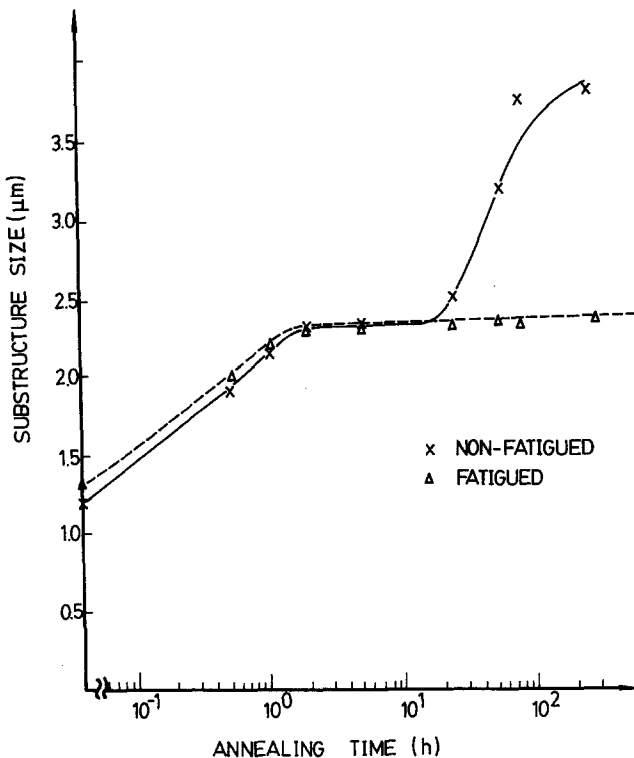


Figure 5 Variation of substructure size with annealing time for specimen S before and after fatigue.

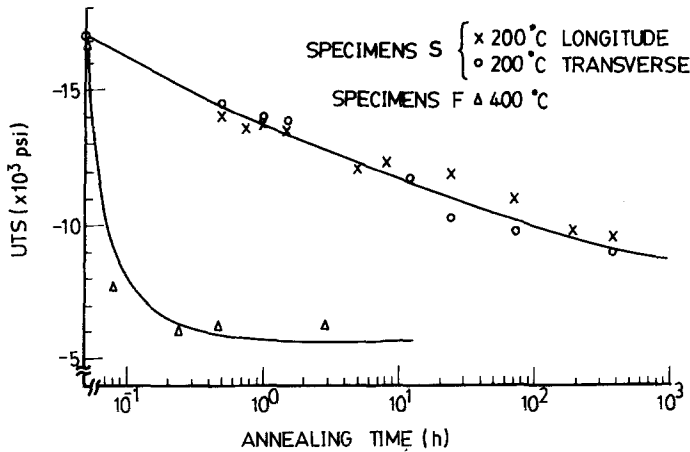


Figure 6 Strength (UTS) versus annealing time for specimens S and F.

strengths if the annealing time is the same. During annealing the microstructure of specimen S changed from dislocation cell with tangle dislocation, to well-defined subgrain (Figs 1a to 4a). However, specimen S did not recrystallize even when the annealing time was as long as 72 h. Since the microstructure of specimens S changed slowly during annealing, the monotonical decrease in the UTS of specimen S can be easily understood.

The UTS of specimen F (annealed at 400°C) dropped significantly for an annealing time of 0 to 0.2 h. When the specimen was annealed at 400°C for more than 0.2 h the UTS decreased very slowly as the annealing time increased. The change of UTS of specimens F can be correlated to the change of their microstructure. Full recrystallization was observed at an annealing time of 0.2 h

at 400°C. After annealing the specimen at 400°C for more than 0.2 h, crystal growth proceeded very slowly. At the stage of recrystallization the UTS of the specimen changed significantly. At the stage of slow crystal growth the UTS of the specimen changed slowly.

The fatigue lives of specimens S and F are plotted in Fig. 7 against their annealing times. Specimens F were fatigued with a stress amplitude of 6×10^3 psi. Specimens S were fatigued with a stress amplitude of 9×10^3 psi or 90% of their ultimate tensile stress. From Fig. 7 we see that the fatigue life of specimen S is much longer than specimen F no matter what the annealing time, even when the stress amplitude of specimen S is 3×10^3 psi larger than that of specimen F. Consequently, the improvement in fatigue property by

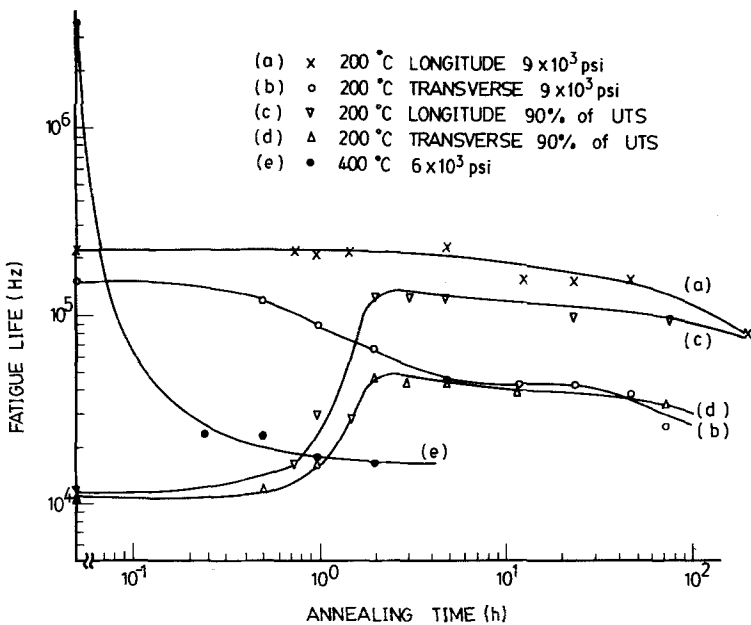


Figure 7 Fatigue lives versus annealing time for specimens S and F.

substructure strengthening in specimen S is appreciable. The fatigue life of specimens S and F decreases monotonically as the annealing time is increased due to the decrease in strength with annealing time. It is worth noting that there exists a peak value of fatigue life of specimen S when the stress amplitude of fatigue is 90% of its ultimate tensile strength. The peak occurs at an annealing time of about 2 h (specimen S 2.0) in which the polygonization of substructure in specimen S is just complete.

Comparing Figs 1b, 2b, 3b and 4b, we find that specimen S 2.0 possesses the most well-defined sub-boundary among specimens S after fatigue. Most sub-boundaries of specimen S 0.0 and S 0.5 after fatigue contain dislocation tangles and there exists a rather high density of dislocations inside the cells. The sub-boundaries of specimen S 7.2 after fatigue also consist of dislocation tangles and some dislocations also exist inside the cells; however, the density is rather low compared to specimens S 0.0 and S 0.5. As shown in Fig. 3b, most sub-boundaries in specimen S 2.0 after fatigue are still very sharp. Although parts of subgrains were changed into dislocation cells (compare Figs 3a and 3b), most subgrains still exist. It is reasonable to assume that fatigue crack propagation prefers to take place along cell boundaries, consisting of dislocation tangles and clusters of dislocation dipoles and loops, than well-defined subgrain boundaries, because the former is with higher stress concentration. This would explain why specimen S 0.2 has the longest fatigue life among all specimens S when fatigued with a stress amplitude of 90% of their ultimate tensile strength.

From Fig. 7 we see that the fatigue life of longitudinal specimen S is always longer than that of transverse specimen S at the same annealing time when the comparison is made at 9×10^3 psi stress amplitude or at a stress amplitude of 90% of its ultimate tensile strength. When the annealing time approaches 100 h the UTS of specimen S is approximately 10 kg mm^{-2} , i.e. 90% UTS = 9×10^3 psi (see Fig. 6). This explains why curves (a) and (c) (also curves (b) and (d)) of Fig. 7 approach each other at an annealing time of about 100 h. The reasons why longitudinal S specimens possess a longer fatigue life than transverse S specimens could be attributed to the texture and mechanical fibering of the specimens. However, further investigation is required for detailed mechanisms.

4. Conclusions

Experimental observations on substructure formation and growth in thermomechanically treated pure aluminium have been made. These specimens, having various pre-existing substructures were then fatigued. The substructures before and after fatigue were compared and then correlated to their fatigue properties. Several conclusions can be drawn.

(1) Well-defined subgrains are formed after annealing the rolled specimens at 200°C for 2 h. The subgrain size remains almost unchanged ($2.32 \mu\text{m}$) until the annealing time reaches 10 h. After that, subgrain size grows by decomposition of weaker sub-boundaries.

(2) Dislocation cells are formed after the specimens are fatigued. The cell boundaries consist of dislocation tangles and/or clusters of dislocation dipoles and loops. The cell size increases initially with annealing time and then reaches a saturation value ($2.32 \mu\text{m}$) when the annealing time is longer than 2 h.

(3) The fatigue life decreases monotonically when the annealing time is increased if the stress amplitude is constant (9×10^3 psi for specimen S, 6×10^3 psi specimen F) due to the decrease in strength. However, when the stress amplitude is 90% of the ultimate tensile strength, the fatigue life of specimen S is longest at an annealing time of 2 h. At this annealing time the specimen possesses subgrains with the sharpest sub-boundaries.

(4) It is suggested that because the well-defined subgrain boundaries possess less stress concentration than the cell boundaries, the fatigue crack propagates more easily along the cell boundaries than along the subgrain boundaries. This would explain why specimen S 2.0 possesses the optimum fatigue property.

References

1. R. J. McELROY and Z. C. SZKOPIAK, *Int. Met. Rev.* 17 (1972) 175.
2. T. J. KOPPENALL, *Trans. ASM.* 62 (1969) 24.
3. C. M. WAN, M. T. JAHN, T. R. YENG, Y. M. LEE and C. T. HU, *J. Mater. Sci.* 11 (1976) 2158.
4. M. T. JAHN, C. M. WAN and T. S. SHEU, *ibid* 13 (1978) 2526.
5. J. G. GROSSKREUTZ and P. WALDOW, *Acta Met.* 11 (1963) 717.
6. M. A. WILKINS and G. C. SMITH, *ibid.* 18 (1970) 18.
7. R. N. GARDNER, T. C. POLLOCK and H. G. F. EILSDORF, *Mater. Sci. Eng.* 29 (1977) 169.
8. M. T. JAHN, TSANN LIN and C. M. WAN, *J. Mater. Sci.* 15 (1980) 1870.

Received 3 July and accepted 10 November 1980.